Noise suppression zeroing neural network for online solving the time-varying inverse kinematics problem of four-wheel mobile manipulators with external disturbances

Zhongbo Sun[1] · Yanpeng Zhou[1] · Shijun Tang[2] · Jun Luo[3] · Bo Zhao[4]

Abstract

A novel noise suppression zeroing neural network (NSZNN) is presented for the trajectory tracking problem on a four Mecanum wheeled mobile manipulator (FMWMM) by solving its time-varying inverse kinematics (TVIK) problem. The holistic kinematic model of the FMWMM is developed, which can receive synergistic control of the mobile manipulator. Different from the situation without external interference addressed in our previous work, this paper considers a variety of common time-varying interferences by studying the basic principles of various noises, and proves the NSZNN model's of the validity and superiority, which solves the TVIK problem of the FMWMM with external disturbances through theoretical analyses. Compared with the existing gradient neural network (GNN) and the traditional zeroing neural network (ZNN), the most representative hybrid noise is selected to conduct a large number of experiments to substantiate the high efficiency and robustness of the NSZNN model. Finally, the NSZNN model is verified on the FMWMM via a robot operating system (ROS) by a successful execution of the trajectory tracking task.

Keywords Noise suppression zeroing neural network · Four Mecanum wheeled mobile manipulator · Inverse kinematics · Time-varying disturbance.

1 Introduction

As a typical model of uncertain complex systems and incompleteness systems (Zhang et al. 2023a; Kong et al. 2021), the trajectory tracking (Khan et al. 2020; Zheng et al. 2022) and path planning (Hentout et al. 2023; Kala et al. 2010) of the Mecanum wheeled mobile manipulator (FMWMM) are the hotspots of the research fields recently. Motion control is the prerequisite for the FMWMM to complete various tasks, and trajectory tracking is the most basic and practical problem in the FMWMM motion control. Therefore, trajectory tracking of the FMWMM has attracted lots of researchers' attention, which is not only widely utilized in industry (Claudia et al. 2021), agriculture (Shangguan et al. 2021), medical treatment (Nguyen et al. 2022), and service (Xi and Zhu 2023), but also in fields of urban security, national defense, space exploration (Liang et al. 2018) and other hazardous domains. Furthermore, an increasing number of algorithms have been exploited and

Extended author information available on the last page of the article

verified to address the trajectory tracking problem of the FMWMM. For example, in Nie et al. (2023), a backstepping and adaptive fuzzy proportion-integral-differential (PID) combining method is presented to solve the trajectory tracking problem of the FMWMM. In Qiu et al. (2019), Qiu et al. develop a nonlinear control law to optimize kinematic and dynamics controllers for the FMWMM with the characteristics of nonlinear, nonholonomic constraint and uncertainty. The authors also introduce integrated feedback technology to decrease the tracking error of the system. In addition, a robust tracking control method is developed for the FMWMM with dynamics and kinematic models, which can compensate for the dynamic uncertainty in the tracking process of the FMWMM and improve the accuracy of trajectory tracking (Jeong and Chwa 2021). Based on above literatures, traditional control algorithms have to establish complex dynamic equations, and are difficult to meet the accurate requirements of the FMWMM trajectory tracking. The combination of traditional control algorithms and the neural network can overcome the aforementioned shortcomings and take the advantages of neural networks to achieve gratifying control results.

Neural networks (Zhang et al. 2023b; Hua et al. 2021; Fu et al. 2021; Sun et al. 2023a; Rajesh 2022, 2023) have broad applications in many fields, such as optimization (Cherupally et al. 2020; Jin et al. 2017), signal processing (Xiang et al. 2020) and pattern recognition (Tan et al. 2019), intelligent control (Machado and Lopes 2017), and fault diagnosis (Zhang et al. 2021). Neural networks and neural dynamics are powerful algorithms to solve many scientific research and engineering problems online (Fu et al. 2020; Zhu et al. 2020; Sun et al. 2019a, b). In Xia et al. (2016), a method of combining the Kalman filter and fuzzy neural network is suggested to solve the trajectory tracking control problem, which improves the efficiency and accuracy of calculation. Recurrent neural networks (RNNs) are a type of neural network, which also contain many neural networks, such as zeroing neural network (ZNN) and primal pairwise neural networks based on linear variational inequalities (Li et al. 2018; Zhang et al. 2018, 2020; Jin et al. 2016).

The RNNs are widely used to solve TVIK problems for mobile manipulators (Li et al. 2018; Zhang et al. 2018, 2020; Jin et al. 2016). In view of the excessive position error of the FMWMM on the trajectory tracking problem, based on the high-order derivative characteristics of noise, a new type of RNN is proposed to eliminate the noise, so as to satisfy the accuracy of the end-effector (EE) (Li et al. 2018). In Zhang et al. (2020), primal pairwise neural network based on linear variational inequalities is widely used in TVIK problems of obstacle avoidance, repetitive motion and trajectory tracking for mobile robotic arms. The primal pairwise neural network based on linear variational inequalities solves the TVIK problem to find a kind of inverse-free solution, which improves the real-time performance. In Jin et al. (2016), an improved ZNN is presented to address the TVIK problem to control the manipulator with exponentially convergent position error, which prove the availability and meliority of neural networks. The presented motion planing of the redundant manipulator had a theoretical analysis of the position error. The orthogonal projection method is introduced to eliminate the position error, and the velocity compensation method with gradient descent function is applied to construct recursive neural networks for the tracking problem of the redundant manipulator (Xie et al. 2020). Benefiting from its linear symbolic bi-power exponential activation function, ZNN possesses good convergence performance to calculate the TVIK problem. The feasibility is further verified by redundant robots (Hu et al. 2021). Aiming at the TVIK of the FMWMM, ZNN can obtain accurate solutions of TVIK problems (Xiao and Zhang 2014). These algorithms are assumed to be free from external interference. However, the position error generated by the calculation is caused by hardware problems or external interference. The Taylor discrete ZNN model adequately considers the time derivative information of time-varying problems but neglects noise (Sun

et al. 2021). In the design of RNN, it is typically assumed that time-varying problems are not subject to external disturbances. However, in the actual experimental hardware implementation process, there are implementation errors and environmental interference, considered as noise. This noise not only significantly impacts the accuracy of RNN solving time-varying problems but may also lead to task failure when precision requirements are high. Additionally, the preprocessing of denoising may introduce additional time, compromising real-time performance. Therefore, it is necessary to explore an improved model that is inherently tolerant to noise and capable of real-time solving of time-varying problems. In order to accurately control FMWMM with different measurement noises, a noise suppression zeroing neural network (NSZNN) model is presented to handle the trajectory tracking of the FMWMM, which is worthy of further investigation. The noise suppression model implemented in this paper can well eliminate external time-varying interference. This is a progress in the control of the FMWMM regarding noise interference, which greatly enhances the stability of the locomotion and manipulation.

The rest of this paper covers the following four directions. The motivation, problem formation, and inverse kinematics (Xiao and Zhang 2014) related problems of the FMWMM are described in Sect. 2. Section 3 proposes and analyzes several types of neural networks, which proves the effectiveness and superiority of the developed NSZNN model compared with the existing models. Section 4 verifies the superiority and robustness of the NSZNN proposed in this paper through a large number of simulations, and proves the effectiveness of the algorithm on robot operating system (ROS) mobile manipulator. Section 5 draws the conclusion and discusses the future works. Finally, the primary contributions of this paper are described as follows.

(1) From the perspective of control, the noise suppression model of the denoising integral term is regarded as a generalized PID controller, and the detailed theoretical analysis and the derivation of the NSZNN model show that the model can effectively solve the TVIK problem.
(2) Based on the external disturbance in the actual application of the FMWMM, a new NSZNN is proposed, which can accurately converge to the inverse kinematics of the FMWMM with noise interference. Numerical results and experiments show that compared with the presented neural network model, the NSZNN model is more effective and accurate in the path-tracking task of the FMWMM.

2 Problem formulation and related work

In order to handle the trajectory tracking problem of the FMWMM involved in the previous section, this section gives the kinematic equations of the manipulator and mobile platform respectively, and integrates them into an overall kinematics equation. The above planning scheme enables the degrees of freedom of the mobile platform to be incorporated into the manipulator system to enhance the overall maneuverability. At the same time, the synergy between the mobile platform and the manipulator motion planning process is ensured.

2.1 The kinematic model of the FMWMM

The FMWMM is shown in Fig. 1a, and it is divided into two parts: the chassis base on four-wheel Mecanum wheels and a four degrees of freedoms (DOFs) manipulator. The vertical
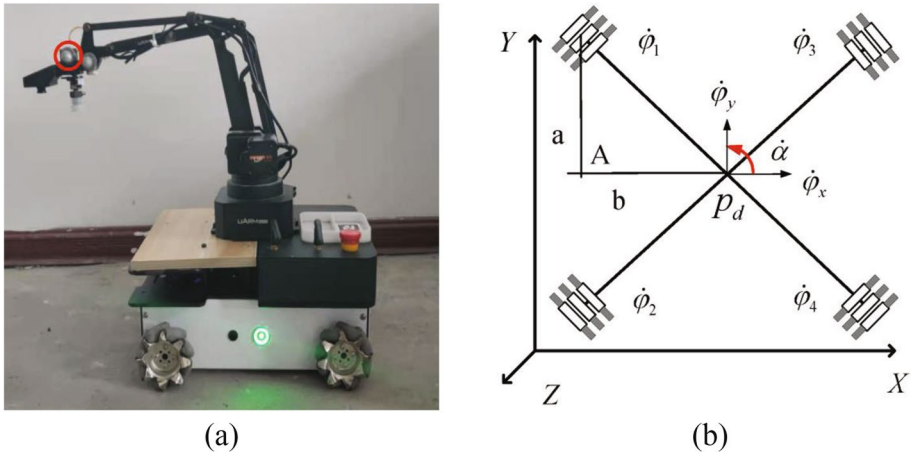
Fig. 1 The FMWMM and its platform model. **a** Physical picture of the FMWMM. **b** Geometric model of mobile platform. (Color figure online)

view of the FMWMM is shown in Fig. 1b, and the relevant parameters are generalized as follows.

(1) P_d: The join point between the manipulator and mobile chassis (x_d, y_d, z_d) with $z_d = 0$.
(2) a: The distance between wheel 1 and point A.
(3) b: The length between the point P_d and point A.
(4) $\dot{\varphi}_x, \dot{\varphi}_y$: The speed of the wheel on the X and Y axes.
(5) α: The velocity of rotation of the mobile platform around point P_d.
(6) $\dot{\varphi}_1, \dot{\varphi}_2, \dot{\varphi}_3, \dot{\varphi}_4$: The velocity of wheel 1, wheel 2, wheel 3 and wheel 4, respectively.

This subsection establishes the kinematic equations of the mobile platform by means of complete constraints on the moving platform. The Mecanum wheel of the moving platform consists of a hub and a roller. The hub is a direct support for the entire wheel, while the roller is a drum mounted on the hub. The angle between the hub axis and the roller axis is 45°. The motion of the moving platform ground is decomposed into three independent parts: X axis translation, Y axis translation and yaw axis rotation. The detailed kinematic modeling derivation of the moving platform can be found in the paper (Sun et al. 2022).

$$
\begin{aligned}
x_d &= -\tfrac{1}{4}\varphi_1 + \tfrac{1}{4}\varphi_2 - \tfrac{1}{4}\varphi_3 + \tfrac{1}{4}\varphi_4 \\
y_d &= \tfrac{1}{4}\varphi_1 + \tfrac{1}{4}\varphi_2 + \tfrac{1}{4}\varphi_3 + \tfrac{1}{4}\varphi_4
\end{aligned}
\tag{1}
$$

The kinematic equation of the FMWMM is expressed as (Xiao and Zhang 2014; Sun et al. 2023b):

$$
f(\mu) = \begin{bmatrix}
\tau_1 c_1 c_2 + \tau_2 c_{23} c_1 + \tau_4 c_{23} c_1 c_4 - \tau_4 s_{23} c_1 s_4 \\
\tau_1 s_1 c_2 + \tau_2 c_{23} s_1 + \tau_4 c_{23} s_1 c_4 - \tau_4 s_{23} s_1 s_4 \\
\tau_2 s_{23} + \tau_1 s_2 + \tau_4 c_{23} s_4 + \tau_4 s_{23} s_4 + \tau_3
\end{bmatrix}
\tag{2}
$$

where μ represents the rotation angle of the manipulator, $c_j := \cos \mu_j$, $s_j := \sin \mu_j$, $c_{23} := \cos(\mu_2 + \mu_3)$ and $s_{23} := \sin(\mu_2 + \mu_3)$ with $j = 1, ..., 4$, $\tau_1 = 0.135$, $\tau_2 = 0.147$, $\tau_3 = 0.103$

and $\tau_4 = 0.035$. Combining (1) with (2), an overall kinematic equation of FMWMM is expressed as follows:

$$\kappa(t) = \begin{bmatrix} x_d \\ y_d \\ 0 \end{bmatrix} + h(\mu, \alpha) \tag{3}$$

where x_d and y_d indicate the location of the mobile platform in the world coordinate system, respectively, and α indicates the rotation angle of the manipulator. The velocity-level kinematic model of FMWMM is constructed as follows:

$$\dot{\kappa}(t) = U\dot{q} \tag{4}$$

where $\dot{\kappa}(t)$ is the temporal differential of the EE location vector of the FMWMM. The coefficient matrix is presented as follows:

$$U = \begin{bmatrix} L & 0 \\ 0 & 0 \end{bmatrix} + J(\alpha, \mu) \begin{bmatrix} P & 0 \\ 0 & I \end{bmatrix}$$

$$P = \frac{1}{4(a+b)}[1, -1, -1, 1]$$

$$L = \begin{bmatrix} -\frac{1}{4} & \frac{1}{4} & -\frac{1}{4} & \frac{1}{4} \\ \frac{1}{4} & \frac{1}{4} & \frac{1}{4} & \frac{1}{4} \end{bmatrix}$$

where Jacobian matrix $J(\alpha, \mu)$ is defined as $J(\alpha, \mu) = \partial h(\alpha, \mu)/\partial \Gamma$; $\Gamma = \left[\mu^\top, \alpha \right]^\top$; I is an identity matrix; $\dot{q} = [\dot{\varphi}, \dot{\mu}^\top]^\top$ delegates the angle velocity vector of the FMWMM, which involves the wheel rotational velocity and the rotational velocity of the manipulator. Note that $b = 0.3$ m, $a = 0.1$ m (Sun et al. 2023b).

2.2 Problem formulation

Due to the disturbance phenomenon in the processing of the trajectory tracking problem of the FMWMM, the NSZNN model is exploited to solve the trajectory tracking problem. When the EE of the FMWMM follows a user-defined trajectory, it is defined as the following case:

$$\Omega(q, t) = \kappa(t) \rightarrow \kappa_d(t) \tag{5}$$

where $\Omega(q, t)$ is a continuous nonlinear positive kinematics mapping of the FMWMM. The EE $\kappa(t)$ of the mobile manipulator is expected to track the desired trajectory κ_d, i.e., $\kappa(t) \rightarrow \kappa_d(t)$. By differentiating Eq. (5) with regard to time t, it can be derived into the following form:

$$U\dot{q} = \dot{\kappa}(t) \rightarrow \dot{\kappa}_d(t) \tag{6}$$

where $\dot{\kappa}_d(t)$ represents the rate of change of the desired trajectory with respect to time t. To be specific, when the FMWMM's EE follows the given trajectory, the corresponding joint angle and wheel velocity are solved in real-time. The above description is the inverse kinematics problem of the FMWMM.

3 NSZNN approach

To address the problems of existing schemes such as inability to deal with noise interference and the existence of hysteresis error, a new NSZNN model is proposed to dispose of the TVIK problem of the FMWMM. At the same time, the NSZNN method and its related models are proposed to suppress the external disturbance to solve the TVIK of the FMWMM. In addition, the detailed theoretical analysis proves the noise-tolerant capability of the presented NSZNN mode.

3.1 NSZNN model

In practical industrial applications, there are many types of disturbances during robot operation, and the NSZNN model and its derivative models are presented to track the trajectory of the FMWMM. A vector-valued error function is defined based on the kinematic equation (4), which makes the NSZNN model limit and drives every item of the error to zero. The expression of the function is shown as follows:

$$\sigma(t) = \kappa_d(t) - \kappa(t) \tag{7}$$

where $\kappa_d(t)$ and $\kappa(t)$ are the anticipant trajectory and practical trajectory of the EE, respectively. For the sake of obtaining an accurate solution, each term of the error function is required to approach zero, and the noise-suppressing zeroing neural dynamic equation is as follows:

$$\dot{\sigma}(t) = -\xi\phi(\sigma(t)) - \delta\int_0^t \sigma(\tau)\mathrm{d}\tau \tag{8}$$

The parameter $\xi > 0$, is set to change the convergence rate of the system, and the parameter $\delta > 0$, ensures the stability of the neural network. $\phi(\cdot)$ is the activation function vector mapping of the neural network, and different types of activation functions are employed to improve the rate of convergence. In this paper, a linear activation function $\phi(\sigma(t)) = \sigma(t)$ is exploited to dispose the noise suppression zeroing neural dynamic model.

Simultaneously process the zeroing neural dynamic system with noise suppression capability and the global kinematics model of the FMWMM, the following expressions can be obtained through calculation:

$$U\dot{q} = \dot{\kappa}_d(t) + \xi\big(\kappa_d(t) - \kappa(t)\big) + \delta\int_0^t \big(\kappa_d(\tau) - \kappa(\tau)\big)\mathrm{d}\tau \tag{9}$$

In addition, the NSZNN model with external disturbances is described as:

$$\dot{q} = U^\dagger(\dot{\kappa}_d(t) + \xi\big(\kappa_d(t) - \kappa(t)\big) + \\ \delta\int_0^t \big(\kappa_d(\tau) - \kappa(\tau)\big)\mathrm{d}\tau + \Upsilon(t)) \tag{10}$$

Algorithm 1: Operational steps of the controller (10)

Input: Desired trajectory κ_d;

Output: Optimized wheel angles φ and joint angles μ;

1: initialize ξ and δ; φ and μ;

2: **repeat**

3: optimize the wheel angles of the mobile platform and the joint angles of the manipulator.

4: observe the positional error $\kappa_d - \kappa$ of the EE and external interference noise $\Upsilon(t)$.

5: refresh the controller state based on $\kappa_d - \kappa$, $\Upsilon(t)$ and the previous state of φ and μ at the last moment.

6: **until** the position of the EE returns to the starting point of the cyclic task.

---

where $\Upsilon(t)$ denotes time-varying disturbance, and $U^\dagger$ is the pseudo-inverse of U. In the actual operation of the FMWMM, there are always external disturbances that affect the normal operation of the robot, for instance, constant external impact interference, transient external force, electromagnetic interference generated by the interaction of current and magnetic field, and continuous random noise or their superposition and so on. Figure 2 demonstrates the composition and basic principles of the neural dynamics equation. The NSZNN algorithm based on temporal derivative information, activation function and integral properties can efficiently solve the trajectory tracking problem of the FMWMM with external disturbances. As shown in Fig. 2, this model is regarded as a representative closed-cycle control system from classical control theory, which is analogous to a control system composed of a generalized PID controller.

3.2 Theoretical analyses

To demonstrate the validity and superiority of the proposed NSZNN model (10) for solving TVIK under time-varying noise (linear noise, sinusoidal noise, exponential decay noise, and continuous bounded random noise), and the strong robustness of NSZNN to different noises is analysed in detail.

Theorem 1 *Consider the existing NSZNN model* (10) *with linear noise disturbances* $\Upsilon(t) = \widehat{\Upsilon}t$. *The NSZNN model is applied to handle the TVIK solution of the FMWMM, and*
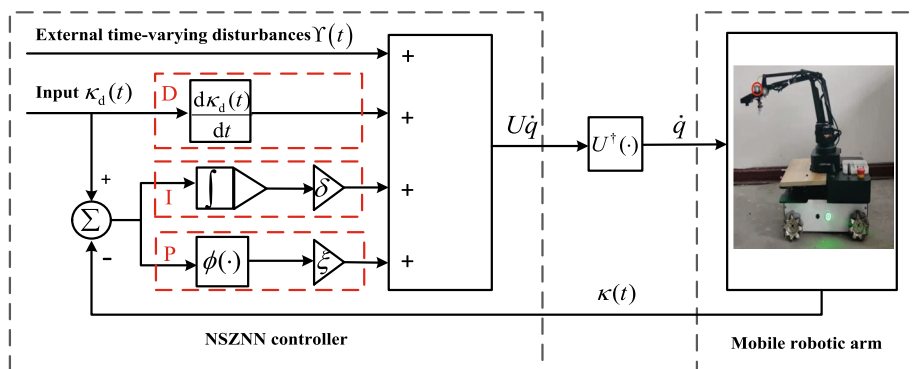

Fig. 2 The control schematic diagram of the NSZNN model

the absolute value of the error of each solution is less than $\lim\limits_{t\to\infty} \left|\sigma_j(t)\right| = \left|\widehat{\Upsilon}_j\right|/\delta$. The absolute value of each error approaches zero as the parameter δ is driven to infinity.

Proof The Laplace transformation of the jth subsystem of the NSZNN model (10) with linear noise is represented as

$$\mathcal{L}\left\{\dot{\sigma}_j(t)\right\} = \mathcal{L}\left\{-\xi\sigma_j(t) - \delta\int_0^t \sigma_j(\tau)\mathrm{d}\tau + \widehat{\Upsilon}_j t\right\} \tag{11}$$

where the symbol $\mathcal{L}\{\cdot\}$ represents the Laplace transformation. Simplifying (11) to get the following form

$$s\sigma_j(s) - \sigma_j(0) = -\xi\sigma_j(s) - \frac{\delta}{s}\sigma_j(s) + \frac{\widehat{\Upsilon}_j}{s^2} \tag{12}$$

where $\frac{\widehat{\Upsilon}_j}{s^2}$ is the Laplace transformation of $\widehat{\Upsilon}_j t$, and the above equation can be converted to

$$\sigma_j(s) = \frac{s\sigma_j(0) + \widehat{\Upsilon}_j}{s(s^2 + \xi s + \delta)} \tag{13}$$

According to the final value theorem (Oppenheim and Willsky 1997), the following equation is obtained as follows:

$$\left|\lim_{t\to\infty}\sigma_j(t)\right| = \left|\lim_{s\to0}s\sigma_j(s)\right| = \left|\lim_{s\to0}\frac{s^2\sigma_j(0) + \widehat{\Upsilon}_j}{s^2 + \xi s + \delta}\right| = \frac{\left|\widehat{\Upsilon}_j\right|}{\delta} \tag{14}$$

$\square$

Remark 1 When the perturbation form is linear, the noise error is driven to zero. From a control-based theoretical viewpoint, the control system is analyzed through the Laplace transformation, which employs a visual and simple graphical method to determine the entire characteristics of the control system. The proposed NSZNN model (10) in this paper performs corresponding theoretical investigation under four common time-varying perturbations, and analyzes the accuracy of the theory on the NSZNN model (10) with external interference by using the Laplace transformation.

Theorem 2 *Consider the developed NSZNN model (10) with sinusoidal time-varying destabilizations, and $\Upsilon(t) = n_j\sin(\vartheta_j(t_j))$. $\vartheta_j \in \mathbb{R}$ and $n_j \in \mathbb{R}$. The NSZNN model (10) converges to an accurate solution of trajectory tracking problem of the FMWMM, and each item has an absolute value of position error $\lim\limits_{t\to\infty}\sigma_j(t) = 0$.*

Proof The Laplace transformation of the jth subsystem of the NSZNN model (10) with sinusoidal time-varying perturbation is represented as

$$\mathcal{L}\{\dot{\sigma}_j(t)\} = \mathcal{L}\left\{-\xi\sigma_j(t) - \delta\int_0^t \sigma_j(\tau)\mathrm{d}\tau + n_j\sin(\vartheta_j(t_j))\right\} \tag{15}$$

Owing to the Laplace transformation, the following equation can be computed as

$$s\sigma_j(s) - \sigma_j(0) = -\xi\sigma_j(s) - \frac{\delta}{s}\sigma_j(s) + \frac{n_j\vartheta_j}{s^2 + \vartheta_j^2} \tag{16}$$

Further, formula (16) can be rewritten as

$$\sigma_j(s) = \frac{s(s^2 + \vartheta_j^2)\sigma_j(0) + sn_j\vartheta_j}{(s^2 + \vartheta_j^2)(s^2 + s\xi + \delta)} \tag{17}$$

Through the final value theorem (Oppenheim and Willsky 1997), it is simplified as

$$\lim_{t\to\infty}\sigma_j(t) = \lim_{s\to 0}\frac{s(s(s^2 + \vartheta_j^2)\sigma_j(0) + sn_j\vartheta_j)}{(s^2 + \vartheta_j^2)(s^2 + s\xi + \delta)} = 0$$

Hereto, the theoretical proof of the NSZNN model (10) with sinusoidal time-varying disturbance is accomplished. □

Theorem 3 *Consider the presented NSZNN model (10) with exponential attenuation interference* $\Upsilon(t) = \zeta_j\exp(-\chi_j t)$. $\zeta \in \mathbb{R}$ *and* $\chi > 0 \in \mathbb{R}$. *The NSZNN model (10) is used to obtain the exact solution of inverse kinematics of the FMWMM with each position error* $\lim_{t\to\infty}\sigma_j(t) = 0$.

Proof The Laplace transformation of the *j*th system of the NSZNN model (10) with an exponential attenuation from disturbance is expressed as

$$\mathcal{L}\{\dot{\sigma}_j(t)\} = \mathcal{L}\left\{-\xi\sigma_j(t) - \delta\int_0^t \sigma_j(\tau)\mathrm{d}\tau + \zeta_j\exp(-\chi_j t)\right\} \tag{18}$$

Simplifying (18) obtains

$$s\sigma_j(s) - \sigma_j(0) = -\xi\sigma_j(s) - \frac{\delta}{s}\sigma_j(s) + \frac{\zeta_j}{s + \chi_j} \tag{19}$$

Then formula (19) is reorganized as

$$\sigma_j(s) = \frac{s(s + \chi_j)\sigma_j(0) + s\zeta_j}{(s + \chi_j)(s^2 + s\xi + \delta)} \tag{20}$$

By means of the final value theorem (Oppenheim and Willsky 1997) to the above equation

$$\lim_{t\to\infty}\sigma_j(t) = \lim_{s\to 0}\frac{s(s(s + \chi_j)\sigma_j(0) + s\zeta_j)}{(s + \chi_j)(s^2 + s\xi + \delta)} = 0$$

The proof is fulfilled. □

Theorem 4 *Consider the acquired NSZNN model* (10) *suffering from continuous bounded time-varying disturbances* $\Upsilon(t)$ *with task time of duration* T_r, *and task execution time* $t \in [0, T_r]$. *The jth item of the system satisfies* $\left|\Upsilon_j(t)\right| \leq \Upsilon_{\max}(t)$ *and* $\Upsilon_{\max}(t) > 0 \in \mathbb{R}$. *External perturbation disappears after the task*, $\Upsilon(t) = 0$ *with* $t > T_r$. *The NSZNN model* (10) *obtains an accurate solution of the TVIK of the FMWMM, and the positional error of each term is* $\lim_{t\to\infty} \sigma_j(t) = 0$.

Proof The Laplace transformation of the *j*th subsystem of the NSZNN model (10) with continuous bounded time-varying perturbation is represented as

$$\mathcal{L}\{\dot{\sigma}_j(t)\} = \mathcal{L}\left\{-\xi\sigma_j(t) - \delta \int_0^t \sigma_j(\tau)\mathrm{d}\tau + \Upsilon_j(t)\right\} \tag{21}$$

Equation (21) can be renewed a simple form

$$s\sigma_j(s) - \sigma_j(0) = -\xi\sigma_j(s) - \frac{\delta}{s}\sigma_j(s) + \int_{-\infty}^{+\infty} \Upsilon_j(t)\exp(-st)\mathrm{d}t \tag{22}$$

Furthermore, the above formula is rewritten as

$$(s + \frac{\delta}{s} + \xi)\sigma_j(s) = \sigma_j(0) + \int_{-\infty}^{+\infty} \Upsilon_j \exp(-st)\mathrm{d}t \tag{23}$$

The above equation simplifies based on the final value theorem (Oppenheim and Willsky 1997) to

$$\left|\lim_{t\to\infty} \sigma_j(t)\right| = \left|\lim_{s\to0} \frac{s^2(\sigma_j(0) + \int_0^{T_r} \Upsilon_j(t)\exp(-st)\mathrm{d}t)}{s^2 + s\xi + \delta}\right|$$
$$\leq \left|\lim_{s\to0} \frac{|s^2|\left|\sigma_j(0)\right| + |s|\left|\Upsilon_{\max}\right|(1 - \exp(-sT_r))|}{|s^2 + s\xi + \delta|}\right| \tag{24}$$
$$= 0$$

Therefore, $\left|\lim_{t\to\infty} \sigma_j(t)\right| = \lim_{t\to\infty} \sigma_j(t) = 0$. The proof is thus fulfilled. $\qquad\square$

Remark 2 The principle analysis of the NSZNN model under different noises shows the necessity of eliminating external disturbances. Specifically, the hardware bias error in the system is treated as a linear disturbance. Electromagnetic interference usually exists during the operation of the FMWMM, which is regarded as the superposition of sinusoidal time-varying interference with an unknown frequency and amplitude. The momentary arc discharge interference generated by the switch closing or cutting off is regarded as an exponential attenuation from a time-varying disturbance. Continuous bounded random noise can represent most of the time-varying disturbances in real life, therefore, it is difficult to express with actual mathematical formulas. The various types of noise discussed above are the principles of the disturbance form of the NSZNN model (10).
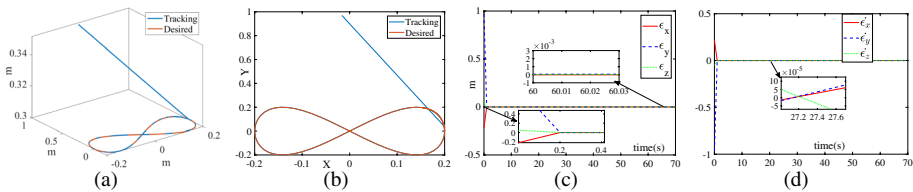
4 Numerical simulations

In this section, numerical simulations certify the efficiency and robustness of the NSZNN model (10) to dispose of the trajectory tracking problem of the FMWMM. The simulation results compare the existing ZNN model (27), gradient neural network (GNN) model (26), and finite-time Zhang neural network (FTZNN) (28), respectively. The results verify the effectiveness of the model proposed in this paper in resisting noise and eliminating hysteresis errors.
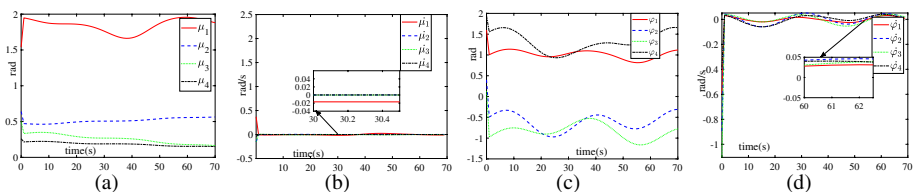
4.1 Numerical results of NSZNN model

In order to prove the noise suppression ability of NSZNN model (10), the advantages and effectiveness of NSZNN model (10) for solving TVIK problems online are verified by the computer simulation, and the simulation time is 70 s. A desired trajectory is provided within an accessible space range, and the FMWMM can move the EE along the desired trajectory. The desired path $\kappa_d(t) = [\kappa_d X(t), \kappa_d Y(t), \kappa_d Z(t)]^\top$ are shown as follows:

$$\begin{cases} \kappa_d X(t) = 0.2 * \cos(0.1t), \\ \kappa_d Y(t) = 0.2 * \sin(0.2t), \\ \kappa_d Z(t) = 0.3. \end{cases} \quad (25)$$

Specifically, initial states of variables are set as $\mu(0) = [0, 0, 0, 0, \pi/3, \pi/3, \pi/3, \pi/3]^\top$ rad, $P_d = \alpha(0) = x_d(0) = y_d(0) = 0$, $\xi = 10$ and $\delta = 300$. Various types of noises are often

Fig. 3 Numerical simulations show the results of utilizing the NSZNN model (10) to control the EE of the FMWMM to track the desired trajectory under hybrid perturbation $\Upsilon(t) = [\exp(-2t); 0.1t; 0.6\sin(3t)]$ and the parameters $\xi = 10$, $\delta = 1000$. **a** The desired trajectory and practical path. **b** Vertical view of the expected path and actual path. **c** Position error. **d** The rate of change of position error

Fig. 4 Numerical simulations show the results of employing the NSZNN model (10) to monitor the EE of the FMWMM to track the desired trajectory under hybrid perturbation $\Upsilon(t) = [\exp(-2t); 0.1t; 0.6\sin(3t)]$ and the parameters $\xi = 10$, $\delta = 1000$. **a** Joint angle of manipulator. **b** Angular speed of manipulator. **c** Angle of mobile platform wheels. **d** Palstance of mobile platform wheels
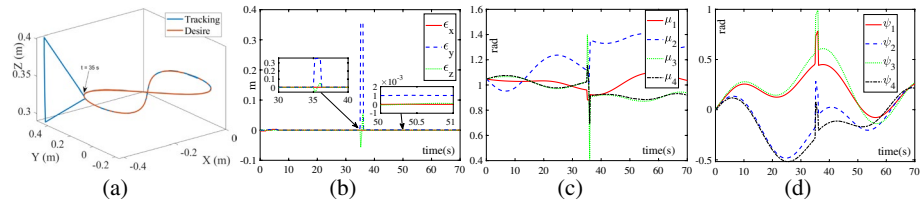
Fig. 5 Numerical simulations show the results of utilizing the NSZNN model (10) to control the EE of the FMWMM to track the desired trajectory under hybrid time-varying destabilization $\Upsilon(t) = [\exp(-2t); 0.1t; 0.6\sin(3t)]$ and parameters $\xi = 100$, $\delta = 1000$. **a** The desired trajectory and practical path. **b** Position error. **c** Joint angle of manipulator. **d** Angle of mobile platform wheels

superimposed in the industrial manufacturing process, and the noise can be regarded as hybrid noise at this time. The noise in Eq. (10) can be simulated using hybrid noise, the specific hybrid noise being $\Upsilon(t) = [\exp(-2t); 0.1t; 0.6\sin(3t)]$. Therefore, the simulation results by using the NSZNN model (10) to control the EE of the FMWMM to track the desired trajectory under time-varying perturbations are shown as follows. Under hybrid noise, the simulation results of the EE tracking the desired trajectory are controlled based on NSZNN model (10), as shown in Figs. 3 and 4. To be specific, as seen from Fig. 3a, it infers that the simulation results of the EE of the FMWMM track the desired trajectory, which reflects the accuracy and rapidity of the control model. Figure 3b is a vertical view, and it can be perceived from Fig. 3 that the actual trajectory of the FMWMM's EE is awfully close to the expected trajectory. Figure 3c reveals the error $\sigma = [\sigma_x, \sigma_y, \sigma_z]^\top$ between the trajectory of the EE of the FMWMM and the expected path. As is depicted from the two partially enlarged images, the NSZNN model (10) quickly converges to zero and possesses a stable performance during the tracking process, which verifies the theoretical proof in Sect. 3. Furthermore, Fig. 3d displays the tracking velocity error of the EE, which shows that the NSZNN model has satisfactory control performance. In addition, the other parametrical variations of the FMWMM's EE while tracking the desired trajectory are shown in Fig. 4a–d. As shown in Fig. 4a, there is no abrupt change in the motion trajectory of each joint of the FMWMM, indicating that the manipulator is stable while tracking the desired trajectory. The angular velocity of the each joint is shown in Fig. 4b, which means the rotation rate of each joint when the FMWMM completes trajectory tracking. During the trajectory tracking process, there is no jitter and vibration in the changes of each joint angle and wheel angle, and the changes of each joint angle and wheel angle are relatively smooth. From Fig. 4b and d, it is obtained that the joint speed and the wheel speed change in a very small range, which further proves that the numerical changes of the manipulator at this moment and the next moment are small, reflecting the stability of the system. At the same time, the motor will not lose data or even be damage due to the excessive numerical change in a short time. It is revealed in the Fig. 4c that the FMWMM changes the velocity of the mobile platform smoothly during the movement, as the data in continuous time relatively less changes and the motor speed also changes smoothly, thus ensuring the completion of the track tracking task. The rotation speed of four wheels on the mobile platform is expressed in Fig. 4d, from which the velocity change of each wheel can be obtained when the FMWMM's EE completes the trajectory tracking task. Simulation results show that the controller always cooperates to monitor the mobile platform and manipulator to fulfill the grasping task of the EE, and demonstrate the efficiency and stability of the NSZNN model (10) proposed to address the trajectory tracking problem of the FMWMM under time-varying disturbances.

In engineering, external interference may not be present at the beginning of trajectory tracking, however, it appears during the tracking process. Therefore it is required that the controller is able to cope with sudden external disturbances. To verify that the NSZNN model has the ability to suppress sudden time-varying noise, the noise is set to appear at time $t = 35$ s in the simulation, and results are shown in Fig. 5. According to Fig. 5b, it can be seen that the error increases rapidly to 0.35 m after the noise appears. Then, the error converges to 0 soon. It indicates that the NSZNN model is able to suppress sudden external disturbances and allows the trajectory tracking error to converge rapidly. In engineering it allows the FMWMM to operate the trajectory tracking task with high accuracy in the environment with the influence of suddenly changing noise.

4.2 Other existing models

In order to attest the efficiency and superiority of the developed NSZNN model (10), a holistic comparison with the existing ZNN model (26) and GNN model (25) is designed. For comparison and discussion, the GNN controller, ZNN controller and NSZNN controller are set to have the same parameters.

In comparison to the previously presented GNN model (Xiao and Zhang 2014): The dynamic equation of the GNN model (25) is shown in (25), which is exploited to compute the inverse of the matrix. In other words, the GNN model (25) can solve the TVIK of the FMWMM. The GNN model (25) with external interference can be represented as the succeeding equation:
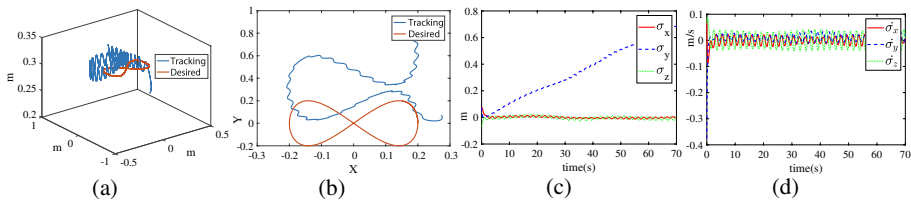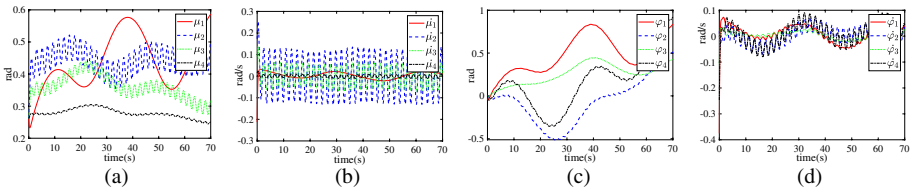

Fig. 6 Numerical simulations show the results of utilizing the GNN model (25) to control the EE of the FMWMM to track the desired trajectory under hybrid time-varying destabilization $\Upsilon(t) = [\exp(-2t); 0.1t; 0.6\sin(3t)]$ and the parameters $\varpi = 10$. **a** The desired trajectory and practical trajectory. **b** Vertical view of the expected trajectory and actual trajectory. **c** Position error. **d** The rate of change of position error
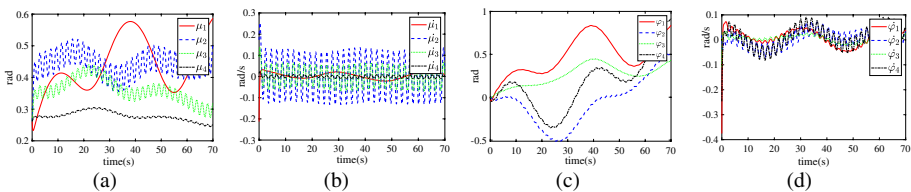
Fig. 7 Numerical simulations show the results of employing the GNN model (25) to solve the EE of the FMWMM to track the desired trajectory under hybrid time-varying destabilization $\Upsilon(t) = [\exp(-2t); 0.1t; 0.6\sin(3t)]$ and the parameters $\varpi = 10$. **a** Joint angle of the manipulator. **b** Joint angle velocity of the manipulator. **c** Angle of mobile platform wheels. **d** Angular velocity of mobile platform wheels
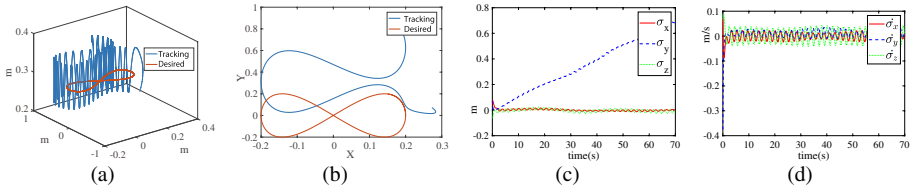
Fig. 8 Numerical simulations show the results of using the ZNN model (26) to manage the EE of the FMWMM to track the desired trajectory under hybrid time-varying destabilization $\Upsilon(t) = [\exp(-2t); 0.1t; 0.6\sin(3t)]$ and the parameters $\xi = 10$. **a** The desired trajectory and practical trajectory. **b** Vertical view of the expected trajectory and actual trajectory. **c** Position error. **d** The rate of change of position error
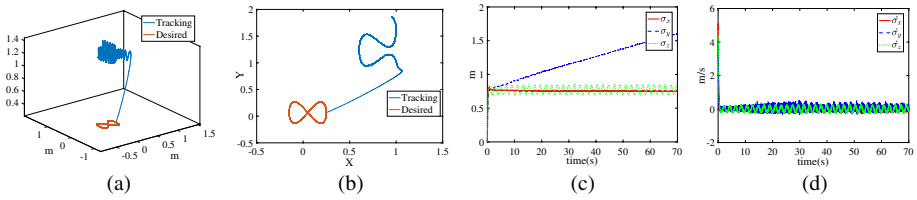

Fig. 9 Numerical simulations show the results of applying the ZNN model (26) to monitor the EE of the FMWMM to track the desired trajectory under hybrid time-varying destabilization $\Upsilon(t) = [\exp(-2t); 0.1t; 0.6\sin(3t)]$ and the parameters $\xi = 10$. **a** Joint angle of the manipulator. **b** Joint angle velocity of the manipulator. **c** Angle of mobile platform wheels. **d** Angular velocity of mobile platform wheels

$$U\dot{q} = \varpi(\kappa_d(t) - \kappa(t)) + \Upsilon(t) \qquad (26)$$

The simulation result of the EE of the FMWMM controlled by the GNN model (25) in tracking the desired trajectory under the disturbance of hybrid noise is shown in Fig. 6a. The desired trajectory and the actual trajectory of the error are large as shown in Fig. 6c, which intuitively shows that the GNN model (25) cannot complete the control task. In summary, the task of tracking the trajectory fails. More details of the trajectory tracking of the FMWMM are shown in Fig. 7. From Fig. 7a–d, the joint variation of the manipulator has buffeting, which indicates that there is a sudden change during the operation, and the wheel velocity variation of the mobile platform also has buffeting, which indicates that there is a mutation in vehicle velocity while tracking the desired trajectory, and it is not allowed in the practical scenarios, which further indicates that the rotational velocity of the mobile platform and the manipulator is unstable in the trajectory tracking. The numerical results infer that the GNN model (25) cannot remove the interference of external. That is to say, the GNN model (25) with external destabilization can not have the effectiveness to dispose the TVIK problem of the FMWMM.

Compared with the current ZNN model (Xiao and Zhang 2014): In the real-time solution process, the derivative information of the coefficient matrix is applied to solve the TVIK problem, that is to say, the ZNN model (26) can obtain a precise value of the TVIK with global exponential convergence. In contrast, the GNN model (25) mentioned in the previous subsection does not use derivative information. It can deal with the trajectory

Fig. 10 Numerical simulations show the results of utilizing the FTZNN model (10) to control the EE of the FMWMM to track the desired trajectory under hybrid perturbation $\Upsilon(t) = [\exp(-2t); 0.1t; 0.6\sin(3t)]$ and the parameters $\xi_1 = \xi_2 = 1, p/q = 0.2$. **a** The desired trajectory and practical trajectory. **b** Vertical view of the expected trajectory and actual trajectory. **c** Position error. **d** The rate of change of position error
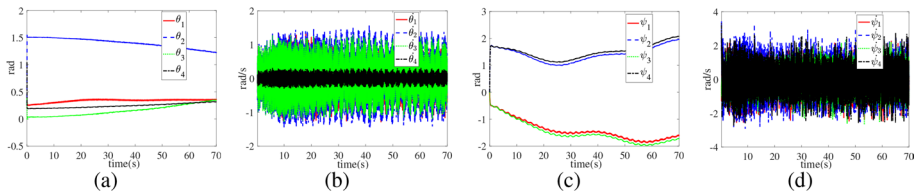
Fig. 11 Numerical simulations show the results of employing the FTZNN model (10) to monitor the EE of the FMWMM to track the desired trajectory under hybrid perturbation $\Upsilon(t) = [\exp(-2t); 0.1t; 0.6\sin(3t)]$ and the parameters $\xi_1 = \xi_2 = 1, p/q = 0.2$. **a** Joint angle of manipulator. **b** Angular speed of manipulator. **c** Angle of mobile platform wheels. **d** Palstance of mobile platform wheels

tracking problem of the FMWMM and the dynamic equation of the ZNN model (26) with external interference is as follows:

$$U\dot{q} = \dot{\kappa}_{\mathrm{d}}(t) + \xi(\kappa_{\mathrm{d}}(t) - \kappa(t)) + \Upsilon(t) \tag{27}$$

Under the interference of hybrid noises, the simulation results of the EE of the FMWMM controlled by the ZNN model (26) while tracking the desired trajectory are shown in Fig. 8a. The ZNN method is still difficult to control the FMWMM to accomplish the trajectory tracking task with the noise interference. The position error of solving the TVIK problem under mixed noise based on ZNN model is shown in Fig. 8c. The divergent position error further proves that the FMWMM cannot accomplish the trajectory tracking. More details of the trajectory tracking of the FMWMM are shown in Fig. 9a–d. From Fig. 9, it can be seen that the curves of the mobile platform and the manipulator have buffeting while completing the trajectory tracking task. If the solved value is sent to the FMWMM, it chatters and will be difficult to complete the track tracking, which is not allowed in practical application. The aforementioned simulation results confirm that the ZNN model (26) cannot eliminate the interference of external time-varying noise. Namely, the ZNN model (26) with external interference can not have the robustness to manage the TVIK problem of the FMWMM. Through the above experiments, it can be seen that, compared with the GNN approach and the ZNN approach, the NSZNN approach has superior performance in solving the TVIK problem with different measurement noises. In addition, in order to demonstrate that the NSZNN model can suppress external noise interference to enable the mobile manipulator to accurately accomplish the trajectory tracking task, the NSZNN model can be used to track the trajectory of the mobile manipulator, the finite-time Zhang

neural network (FTZNN) model (Xiao et al. 2018) is compared and analyzed with the NSZNN in this paper. The FTZNN model is constructed as follows.

$$U\dot{q} = \dot{\kappa}_d(t) + \xi_1(\kappa_d(t) - \kappa(t))$$
$$+ \xi_2(\kappa_d(t) - \kappa(t))^{p/q} + \Upsilon(t) \tag{28}$$

where the parameters $\xi_1 = \xi_2 = 1, p/q = 0.2$, and hybrid perturbation $\Upsilon(t) = [\exp(-2t); 0.1t; 0.6\sin(3t)]$. Numerical simulations show the results of utilizing the FTZNN model (11) to control the EE of the FMWMM to track the desired trajectory under hybrid perturbation $\Upsilon(t) = [\exp(-2t); 0.1t; 0.6\sin(3t)]$ and the parameters $\xi_1 = \xi_2 = 1$. From Fig. 10a–d, it can be obtained that the FTZNN model cannot control the mobile machinery to track the desired trajectory in the presence of noisy interference. From Fig. 11a–d, it is obtained that the error becomes dispersion form with time and the position error increases to 1.5 m. Thus, the FTZNN model cannot suppress the external noise to accurately interfere with the completion of the trajectory tracking task. In addition, the FTZNN model does not satisfy the Lipschitz continuity requirement for some activation functions (Liu and Shang 2022). Especially in noisy environments, the FTZNN model makes it very difficult for mobile manipulators to accurately perform trajectory tracking tasks. Therefore, it is very difficult to achieve finite-time convergence of models equipped with these types of activation functions in practice.

Analyzed from the perspective of control in conjunction with Fig. 2, the NSZNN model (10) can be regarded as a generalized PID controller, which combines the desired temporal derivative and integral terms. The GNN model (25) and ZNN model (26) can be regarded as generalized P controller and PD controller respectively. The P controller has the effect of fast adjustment, but the error cannot be eliminated without the integral term. The PD controller has a differential term, which can predict the error trend and improve the dynamic performance of the system, but it has an amplification effect on noise interference and leads to system instability. However, the PID controller not only has the ability of rapid adjustment and advanced control to eliminate deviations, but also has an integral term that eliminates the steady-state error of the system and eliminates the influence of external noise on the system. Therefore, the NSZNN model (10) controller is more effective and superior in dealing with TVIK problems.

4.3 Comparison of different parameters

To testify the meliority and effectiveness of the NSZNN model (10) in solving the TVIK problem of the FMWMM with various noises, the same type noise is selected for comparison. According to the root mean square error of position in Table 1, it can be clearly judged that the position error of the EE of the FMWMM controlled by the NSZNN model (10) in tracking the desired trajectory is less than that of the other two models under the three kinds of noises. Therefore, the NSZNN model (10) is more splendid than the GNN model (25) and ZNN model (26) in TVIK problems of the FMWMM with noises polluted.

Table 1 Comparison of NSZNN model (10), ZNN model (26) and GNN model (25) of the root mean square error of the EE position under different noises

| Controller/noise type	Linear noise	Sinusoidal noise	Hybrid noise
GNN	1.007×10^{-1}	1.100×10^{-3}	2.900×10^{-3}
ZNN	3.510×10^{-2}	3.892×10^{-4}	3.899×10^{-4}
NSZNN	1.558×10^{-4}	9.776×10^{-6}	9.190×10^{-6}
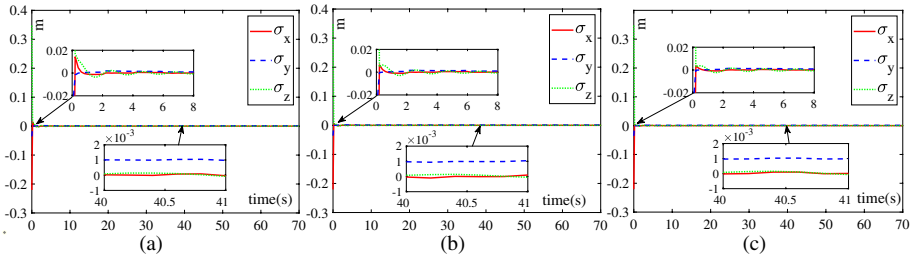
Fig. 12 The position error of the FMWMM's EE of the NSZNN model under different parameters while tracking the desired trajectory with $\delta = 100$. **a** $\xi = 10$. **b** $\xi = 50$. **c** $\xi = 100$

Table 2 Root-mean-square error of the position of X-axis, Y-axis and Z-axis of the FMWMM controlled by the NSZNN model with different parameters under $\delta = 100$

Parameter ξ	σ_x	σ_y	σ_z
10	1.1798×10^{-2}	2.1556×10^{-3}	1.8578×10^{-2}
50	1.1775×10^{-2}	2.1410×10^{-3}	1.8545×10^{-2}
100	1.1772×10^{-2}	2.1311×10^{-3}	1.8540×10^{-2}
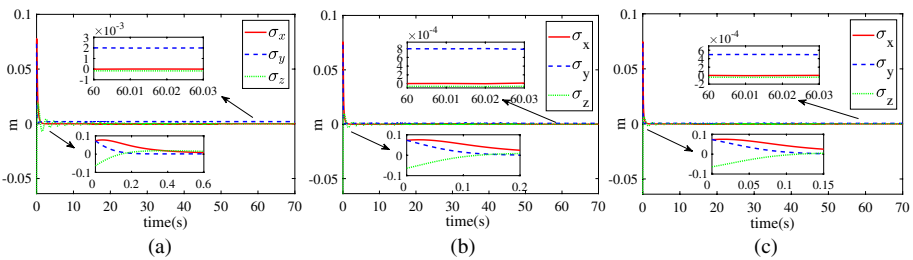
Fig. 13 The position error of the FMWMM's EE of the NSZNN model (10) under different parameters while tracking the desired trajectory with $\xi = 10$. **a** $\delta = 50$. **b** $\delta = 125$. **c** $\delta = 200$

Table 3 Root-mean-square error of the position of X-axis, Y-axis and Z-axis of the FMWMM controlled by the NSZNN model (10) with different parameters under $\xi = 10$

Parameter δ	σ_x	σ_y	σ_z
50	3.4912×10^{-4}	2.0000×10^{-3}	5.3641×10^{-5}
125	2.2919×10^{-4}	8.6327×10^{-4}	8.3252×10^{-6}
200	1.8065×10^{-4}	5.5958×10^{-4}	5.6559×10^{-6}

The parameters of the NSZNN model are modified to alter the convergence rate and error accuracy of the system. The simulation results for different sizes of parameter ξ are shown in Fig. 12 and Table 2, where the parameter is $\delta = 100$. It can be informed by Fig. 12 that as the parameter ξ increases, the smaller the error fluctuates in the initial stage, and the faster the convergence is. This indicates that the larger the parameter ξ is, the faster the NSZNN model converges. Meanwhile, Table 2 shows that the larger the parameter ξ, the smaller the error, which is due to the fact that faster convergence of the system results in the error remaining lower

Table 4 Comparison of different controllers for mobile manipulator motion

Scheme	Mobile or fixed-based or no	Error accumulation elimination	Error derivation	Platform verification	Scheme level	Noise suppression
NSZNN	Both	$\surd$	$\surd$	$\surd$	Velocity-level	$\surd$
GNN (25)	Fixed-based	×	×	×	Velocity-level	×
ZNN (26)	Mobile	×	×	×	Velocity-level	×
Sun et al. (2019a)	No	$\surd$	$\surd$	×	No	×
Zhang et al. (2020)	Mobile	×	×	×	Velocity-level	×
Xie et al. (2020)	Fixed-based	×	×	×	Velocity-level	×
Sun et al. (2022)	Both	×	×	×	Velocity-level	×
Xiao et al. (2018)	No	×	×	×	No	×
Sun et al. (2023c)	Both	$\surd$	$\surd$	×	Velocity-level	$\surd$

for more time, resulting in a smaller trajectory tracking error. Therefore, the desired tracking effect can be achieved by appropriately adjusting the parameter ξ under actual conditions.

Compared the NSZNN model with different parameters δ to change the convergence velocity of the inverse kinematics of the FMWMM. It can be received from Fig. 13, where the parameter is $\xi = 10$. As the noise coefficient increases, the convergence speed of the system increases. The convergence time of the system at $\delta = 200$ is faster than that at $\delta = 50$. Namely, the convergence ratio can be manually controlled by changing the parameter δ of the NSZNN model (10). Combining Fig. 13 and Table 3, it can be concluded that as the parameter δ increases, the stability of the system can be increased. Table 3 intuitively shows that as the parameter δ becomes larger, the position error of the FMWMM's EE while tracking the desired trajectory in each coordinate axis is significantly reduced. In summary, noise suppression can quickly reduce the trajectory tracking error and quickly reduce the effect of external disturbances. Therefore it can also affect the convergence of the system. When the parameter δ is increased, the error is reduced and the convergence is improved. In actual conditions, the effect of the desired tracking can be achieved by appropriately adjusting the parameter δ.

In addition, the results of the different schemes comparison are summarized in Table 4. To emphasize the superiority of the NSZNN model (10), many studies of mobile manipulators (Zhang et al. 2020; Xie et al. 2020; Sun et al. 2019a, 2022, 2023c; Xiao et al. 2018) in recent years have compared with the NSZNN (10) model, and the results are presented in Table 4. First, the proposed NSZNN model is feasible for both the fixed and mobile manipulators. This illustrates the wide applicability of the NSZNN model (10). Second, the NSZNN model (10) can solve the time-varying nonlinear system of equations problem accurately under noise pollution and adjust the error from large values to zero, while some models cannot. Third, only the NSZNN model (10) is validated on a platform, while other models are not validated on a platform. Thus, the superior performance of the NSZNN model (10) is illustrated based on the above advantages.

4.4 Mobile manipulator experiments

In order to verify the validity and stability of the NSZNN algorithm, a further test is conducted on a physical mobile manipulator. The algorithm verification principle block diagram is shown in Fig. 14. The optical motion capture system produced by NOKOV is used
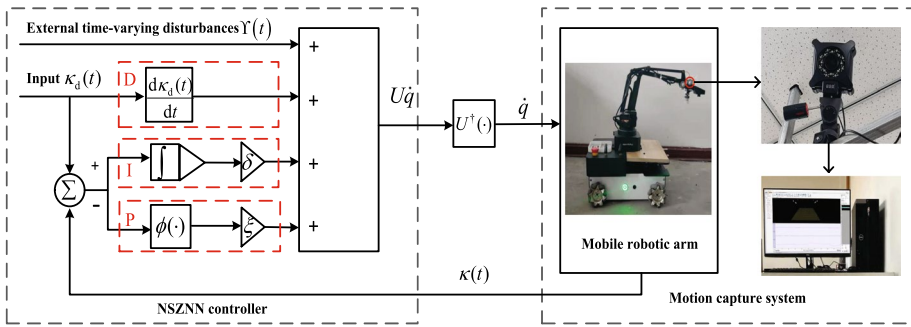
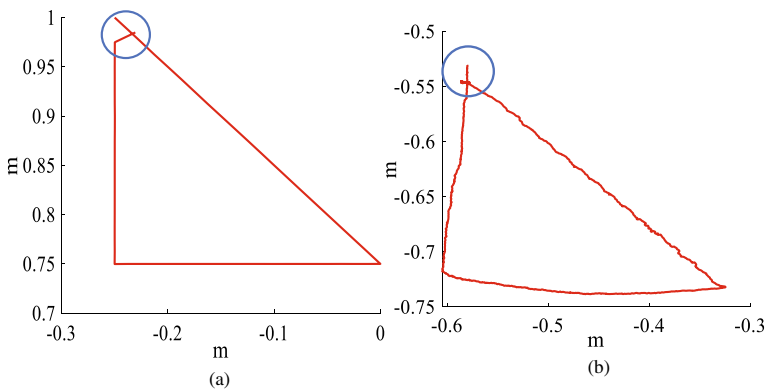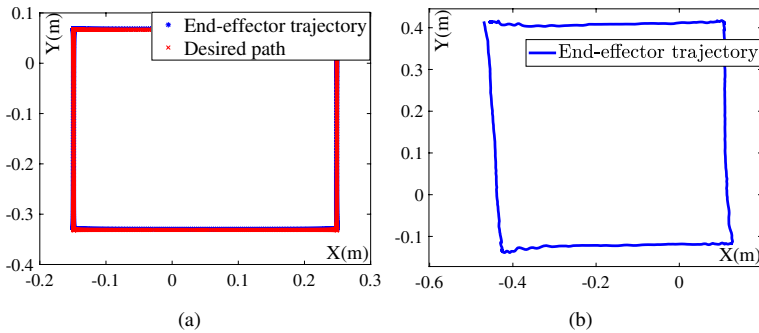**Fig. 14** Algorithm validation schematic block diagram

Fig. 15 MATLAB simulation tracking diagram and ROS based mobile manipulator actual tracking diagram. **a** The trajectory tracking diagram based on MATLAB simulation. **b** The trajectory tracking curve based on ROS mobile manipulator

to capture the position of the Marker point (the point in the red circle in Fig. 1a) of the ROS mobile manipulator's EE in 3D space real-timely. First, the data archive profile is created and loaded using the Seeker software. Second, connect the workstation to the lens and change the workstation page layout, which allows the top of the page to place the connected lens area and the bottom half of the page to be the data capture area. Third, mark the end-effector positions of the FMWMM as marker points and place them in the center of the motion capture field. Fourth, other stray and reflective points are dealt with in the 2D view to ensure the accuracy and reliability of the data acquisition environment. The collected data are drawn with MATLAB, and the effectiveness of the algorithm has been verified by comparison with expected the trajectory.

　　Figure 15 shows the desired trajectory computed by MATLAB and the actual trajectory returned by the optical motion capture system. It is illustrated in the Fig. 15a that giving the initial state point in MATLAB is difficult to satisfy the expected trajectory equation, so in the initial stage of trajectory tracking, the EE in Fig. 15a is difficult to track the expected trajectory, which is partly marked in the blue circle in Fig. 15a. During the operation of the ROS mobile manipulator, there is a large gap between the rotational speed of the mobile platform and the manipulator after receiving the command. For example, when the robot

Fig. 16 MATLAB simulation tracking diagram and ROS based mobile manipulator actual tracking diagram. **a** The trajectory tracking diagram based on MATLAB simulation. **b** Actual tracking trajectory of a mobile manipulator based on a motion capture system

terminal issues the instruction of wheel rotation at a fixed angle, the wheel rotates rapidly to a specified angle. The rotation angle instruction is sent to the manipulator through the terminal, and the rotational speed of the manipulator is very slow. Therefore, in order to overcome the limitation of slow rotation speed of the manipulator, a delay of 60 s is added to the C++ program in this paper to make the manipulator move to the expected initial position. In the initial stage, there is no trajectory curve turning similar to Fig. 15a in b, and the starting position is on the expected trajectory, namely the blue circle in Fig. 15b.

In addition, it is considered that no delay command is added in C++, but there is a large difference between the rotational speed of the manipulator and that of the mobile platform within a certain time, which will lead to greater initial position error and failure of the trajectory task over time. ROS mobile manipulator weighs 10 kg. When the whole C++ program runs to the final stage, the value sent to each motor is small, and the power generated by motor rotation is not enough to overcome the weight of the FMWMM itself, so it is difficult to return to the starting position. As can be seen from Fig. 15b, the moving manipulator tracks the triangle in counterclockwise direction, and NSZNN algorithm is effective and can control the EE to complete trajectory tracking in general. However, the trajectory tracking curve in Fig. 15b still has a lot of jitters, which needs to be improved in the future.

The NSZNN model proposed in this paper is essentially a solution to the time-varying nonlinear system of equations problem, a time-varying quadratic programming scheme for the mobile manipulator tracking a square trajectory is illustrated by an example to verify that the mobile manipulator tracks a square trajectory without jitter. The time-varying quadratic programming problem of the mobile manipulator can be converted to a time-varying nonlinear system of equations problem by the Karush–Kuhn–Tucker condition. The NSZNN model solves the time-varying quadratic programming problem platform experiment as shown in Fig. 16. In the experiment, mobile manipulator EE is expected to trace a rectangular trajectory. The Fig. 16 shows the numerical tracking results of the mobile manipulator and the actual trajectory based on the optical motion capture system, respectively. From Fig. 16a and b it can be obtained that the NSZNN model is valid to enable the mobile manipulator to accomplish the trajectory tracking task. The Fig. 16b illustrates the experimental results of mobile manipulator synthesized by time-varying quadratic programming with equation and inequality constraints, which were solved using the NSZNN model. These experimental results confirm the physical realizability of the NSZNN model

in solving time-varying quadratic programming with equation and inequality constraints with noise.

5 Conclusion

A superior NSZNN model based on the classic ZNN model has been proposed to solve the TVIK problem. The TVIK problem of the FMWMM with various time-varying perturbations has been analyzed and the results show that the NSZNN model can quickly converge to the exact solution of the TVIK, and the reason of its noise suppression capability has been analyzed from the control point of view. In addition, the simulation results has shown that NSZNN model has advantages over GNN model and ZNN model, which also have reflected that NSZNN model has faster convergence performance by adjusting parameters. Ultimately, the effectiveness of the algorithm has been verified on the ROS mobile manipulator platform. In future research, we will introduce the ZNN model with nonconvex activation function to solve the time-varying nonconvex constrained optimization problem.

Data availability No datasets were generated or analysed during the current study.

Declarations

Competing interests The authors declare no competing interests.

References

Cherupally SK, Yin S, Kadetotad D, Srivastava G, Bae C, Kim SJ (2020) ECG authentication hardware design with low-power signal processing and neural network optimization with low precision and structured compression. IEEE Trans Biomed Circuits Syst 14(2):198–208

Claudia G, Ernesto SJ, Adolfo M, Luis G, Luis G (2021) Advanced teleoperation and control system for industrial robots based on augmented virtuality and haptic feedback. J Manuf Syst 59:283–298

Fu J, Tian F, Chai T, Jing Y, Li Z, Su C-Y (2020) Motion tracking control design for a class of nonholonomic mobile robot systems. IEEE Trans Syst Man Cybern Syst 50(6):2150–2156

Fu Y, Jin L, Xu J, Xiao X, Fu D (2021) Reformative noise-immune neural network for equality-constrained optimization applied to image target detection. IEEE Trans Emerg Top Comput 10(2):973–984

Hentout A, Maoudj A, Aouache M (2023) A review of the literature on fuzzy-logic approaches for collision-free path planning of manipulator robots. Artif Intell Rev 56:3369–3444

Hu Z, Xiao L, Li K, Li K, Li J (2021) Performance analysis of nonlinear activated zeroing neural networks for time-varying matrix pseudoinversion with application. Appl Soft Comput 98:106735

Hua C, Jiang A, Li K (2021) Adaptive neural network finite-time tracking quantized control for uncertain nonlinear systems with full-state constraints and applications to QUAVs. Neurocomputing 440:264–274

Jeong S, Chwa D (2021) Sliding-mode-disturbance-observer-based robust tracking control for omnidirectional mobile robots with kinematic and dynamic uncertainties. IEEE/ASME Trans Mechatron 26(2):741–752

Jin L, Zhang Y, Li S, Zhang Y (2016) Modified ZNN for time-varying quadratic programming with inherent tolerance to noises and its application to kinematic redundancy resolution of robot manipulators. IEEE Trans Ind Electron 63(11):6978–6988

Jin L, Li S, La H, Luo X (2017) Manipulability optimization of redundant manipulators using dynamic neural networks. IEEE Trans Ind Electron 64(6):4710–4720

Kala R, Shukla A, Tiwari R (2010) Fusion of probabilistic A* algorithm and fuzzy inference system for robotic path planning. Artif Intell Rev 33:307–327

Khan AH, Li S, Chen D, Liao L (2020) Tracking control of redundant mobile manipulator: an RNN based metaheuristic approach. Neurocomputing 400:272–284

Kong L, He W, Dong Y, Cheng L, Yang C, Li Z (2021) Asymmetric bounded neural control for an uncertain robot by state feedback and output feedback. IEEE Trans Syst Man Cybern Syst 51(3):1735–1746

Li S, Wang H, Rafique MU (2018) A novel recurrent neural network for manipulator control with improved noise tolerance. IEEE Trans Neural Netw Learn Syst 29(5):1908–1918

Liang Z, Chen J, Wang Y, Ding L, Gao H, Deng Z (2018) Approach for imitation of manned lunar rover acceleration using a prototype vehicle with imitation handling ratio on the earth. IEEE Trans Veh Technol 67(7):5683–5694

Liu M, Shang M (2022) On RNN-based k-WTA models with time-dependent inputs. IEEE/CAA J Autom Sin 9(11):2034–2036

Machado JT, Lopes AM (2017) A fractional perspective on the trajectory control of redundant and hyper-redundant robot manipulators. Appl Math Model 46:716–726

Nguyen T, Bui T, Pham H (2022) Using proposed optimization algorithm for solving inverse kinematics of human upper limb applying in rehabilitation robotic. Artif Intell Rev 55(3):679–705

Nie J, Wang Y, Mo Y, Miao Z, Jiang Y, Zhong H, Lin J (2023) An HQP-based obstacle avoidance control scheme for redundant mobile manipulators under multiple constraints. IEEE Trans Ind Electron 70(6):6004–6016

Oppenheim AV, Willsky AS (1997) Signals and systems. Prentice-Hall, Englewood Cliffs

Qiu Y, Li B, Shi W, Zhang X (2019) Visual servo tracking of wheeled mobile robots with unknown extrinsic parameters. IEEE Trans Ind Electron 66(11):8600–8609

Rajesh K (2022) A Lyapunov-stability-based context-layered recurrent pi-sigma neural network for the identification of nonlinear systems. Appl Soft Comput 122:108836

Rajesh K (2023) Memory recurrent Elman neural network-based identification of time-delayed nonlinear dynamical system. IEEE Trans Syst Man Cybern Syst 53(2):753–762

Shangguan L, Thomasson JA, Gopalswamy S (2021) Motion planning for autonomous grain carts. IEEE Trans Veh Technol 70(3):2112–2123

Sun Z, Shi T, Wei L, Sun Y, Liu K, Jin L (2019a) Noise-suppressing zeroing neural network for online solving time-varying nonlinear optimization problem: a control-based approach. Neural Comput Appl 32:11505–11520

Sun Z, Li F, Zhang B, Sun Y, Jin L (2019b) Different modified zeroing neural dynamics with inherent tolerance to noises for time-varying reciprocal problems: a control-theoretic approach. Neurocomputing 14:165–179

Sun Z, Shi T, Jin L, Zhang B, Pang Z, Yu J (2021) Discrete-time zeroing neural network of pattern for online solving time-varying nonlinear optimization problem: application to manipulator motion generation. J Franklin Inst 358(14):7203–7220

Sun Z, Tang S, Zhou Y, Yu J, Li C (2022) A GNN for repetitive motion generation of four-wheel omnidirectional mobile manipulator with nonconvex bound constraints. Inf Sci 607:537–552

Sun Y, Cao J, Sun Z, Tang S (2023a) A nonconvex function activated noise-tolerant neurodynamic model aided with Fischer-Burmeister function for time-varying quadratic programming in the presence of noises. Neurocomputing 520:365–375

Sun Z, Tang S, Jin L, Zhang J, Yu J (2023b) Nonconvex activation noise-suppressing neural network for time-varying quadratic programming: application to omnidirectional mobile manipulator. IEEE Trans Ind Inform. https://doi.org/10.1109/TII.2023.3241683

Sun Z, Shi T, Zhang J, Yu J (2023c) Nonconvex noise-tolerant neural model for repetitive motion of omnidirectional mobile manipulators. IEEE/CAA J Autom Sin 10(8):1766–1768

Tan Z, Li W, Xiao L, Hu Y (2019) New varying-parameter ZNN models with finite-time convergence and noise suppression for time-varying matrix Moore-Penrose inversion. IEEE Trans Neural Netw Learn Syst 31(99):2980–2992

Xi X, Zhu S (2023) A comprehensive review of task understanding of command-triggered execution of tasks for service robots. Artif Intell Rev 56:7137–7193

Xia K, Gao H, Ding L, Liu G, Deng Z, Liu Z, Ma C (2016) Trajectory tracking control of wheeled mobile manipulator based on fuzzy neural network and extended Kalman filtering. Neural Comput Appl 30:447–462

Xiang H, Chen B, Yang T, Liu D (2020) Improved de-multipath neural network models with self-paced feature-to-feature learning for DOA estimation in multipath environment. IEEE Trans Veh Technol 69(5):5068–5078

Xiao L, Zhang Y (2014) Solving time-varying inverse kinematics problem of wheeled mobile manipulators using Zhang neural network with exponential convergence. Nonlinear Dyn 76:1543–1559

Xiao L, Liao B, Li S, Zhang Z, Ding L, Jin L (2018) Design and analysis of FTZNN applied to the real-time solution of a nonstationary Lyapunov equation and tracking control of a wheeled mobile manipulator. IEEE Trans Ind Inform 14(1):98–105

Xie Z, Jin L, Luo X, Sun Z, Liu M (2020) RNN for repetitive motion generation of redundant robot manipulators: an orthogonal projection-based scheme. IEEE Trans Neural Netw Learn Syst 33(2):615–628

Zhang Y, Li S, Gui J, Luo X (2018) Velocity-level control with compliance to acceleration-level constraints: a novel scheme for manipulator redundancy resolution. IEEE Trans Ind Inform 14(3):921–930

Zhang Z, Chen S, Zhu X, Yan Z (2020) Two hybrid end-effector posture-maintaining and obstacle-limits avoidance schemes for redundant robot manipulators. IEEE Trans Ind Inform 16(2):754–763

Zhang K, Chen J, He S, Xu E, Li F, Zhou Z (2021) Differentiable neural architecture search augmented with pruning and multi-objective optimization for time-efficient intelligent fault diagnosis of machinery. Mech Syst Signal Process 158(7):107773

Zhang X, Xu T, Zhang Z, Duan Z (2023a) Parallel extended state observer based control for uncertain nonlinear systems. Neurocomputing 557:126687

Zhang J, Li C, Yin Y, Zhang J, GrzegorzekC M (2023b) Applications of artificial neural networks in microorganism image analysis: a comprehensive review from conventional multilayer perceptron to popular convolutional neural network and potential visual transformer. Artif Intell Rev 56:1013–1070

Zheng Y, Liu Y, Song R, Ma X, Li Y (2022) Adaptive neural control for mobile manipulator systems based on adaptive state observer. Neurocomputing 489:504–520

Zhu W, Guo X, Fang Y, Zhang X (2020) A path-integral-based reinforcement learning algorithm for path following of an autoassembly mobile robot. IEEE Trans Neural Netw Learn Syst 31(11):4487–4499

Authors and Affiliations

Zhongbo Sun[1] · Yanpeng Zhou[1] · Shijun Tang[2] · Jun Luo[3] · Bo Zhao[4]

✉ Bo Zhao
zhaobo@bnu.edu.cn

Zhongbo Sun
zbsun@ccut.edu.cn

Yanpeng Zhou
2201904036@stu.ccut.edu.cn

Shijun Tang
2202004067@stu.ccut.edu.cn

Jun Luo
303756981@qq.com

[1] Department of Control Engineering, Changchun University of Technology, Changchun 130012, China

[2] Department of Communication Engineering, Jilin University, Changchun 130025, China

[3] Vehicle Test Center, Chongqing SERES New Energy Vehicle Design Institute Co., Ltd., Chongqing 401135, China

[4] School of Systems Science, Beijing Normal University, Beijing 100875, China